JOURNAL OF CATALYSIS **92**, 136–144 (1985)

Morphological Characterization of Etched Metal Catalysts

R. J. WILLEY,[1] W. C. CONNER, AND J. W. ELDRIDGE

Department of Chemical Engineering, University of Massachusetts, Amherst, Massachusetts

Received August 1, 1984; revised October 31, 1984

Etched metal catalysts, 430 stainless-steel wire mesh diffusion coated with aluminum which is subsequently leached away, have been found very active for the reduction of NO by NH_3. Presented here is characterization work showing the dramatic surface roughening created by this preparation process. Microprobe studies show that a counter diffusion process takes place in which aluminum diffuses into the surface while iron and chromium diffuse out. There is suggestion that two iron/aluminum phases exist similar to a Raney nickel (J. Freel, W. J. M. Pieters, and R. B. Anderson, *J. Catal.* **16,** 218, 1970). Comparison of the fully leached etched metal catalyst to other deNO$_x$ catalysts show it to have one of the highest activities yet seen, on a basis of active surface area as opposed to total weight. © 1985 Academic Press, Inc.

INTRODUCTION

A novel catalyst preparation method patented by Baldi and Damiano (*2*) has produced a catalyst that is extremely reactive toward the selective catalytic reduction of NO by NH_3 (*3*). The purpose of this paper is to present results of morphological characterization of these etched metal catalysts.

Etched metal catalysts are formed by a diffusional coating process in which a low melting point metal such as aluminum or zinc is diffused into a metallic or alloy surface such as nickel or stainless steel. The process is further described in the literature (*4, 5, 6*). After diffusing such metal, say aluminum, into the surface, it is leached away by an alkali to form an activated catalyst. The process is very similar to that for Raney nickel or cobalt except that aluminum is coated onto the outside of the alloy versus being part of it, and that the alloy of interest is 430 stainless steel, composed of 80% iron and 20% chromium. Also, these screens are not pyrophoric.

In this study, 430 SS wire screen (18 mesh—0.017-in.-diameter wire) was subjected to the above process to form an extremely active catalyst for the reaction of

$$NO + NH_3 + \tfrac{1}{4}O_2 \rightarrow N_2 + \tfrac{3}{2}H_2O \quad (1)$$

The rigid wire mesh form of these catalysts is attractive because it can easily be fabricated into low pressure drop reactor configurations.

Porosimetry, scanning electron microscopy, and scanning elemental microprobing were used to assist in gaining fundamental understanding of what etched metal surfaces comprise and what leads to their high activity. Further characterization was done with a multipoint BET to determine the surface areas.

EXPERIMENTAL

Surface area measurements were made with a conventional volumetric BET apparatus. One to two grams of activated wire mesh were cut into pieces to fit into the 1-cm-diameter sample vial. The severed ends did not contribute significantly to the surface area.

Samples for the scanning electron microscope (SEM) were made by clipping single wire segments from the wire mesh catalyst and mounting them onto an aluminum sample holder with graphite. Since the wires

---

[1] Present address: Department of Chemical Engineering, Northeastern University, Boston, Massachusetts.

0021-9517/85 $3.00
Copyright © 1985 by Academic Press, Inc.
All rights of reproduction in any form reserved.

TABLE 1

Etched Metal Catalysts Characterized

Etched metal catalyst		BET surface area, m^2/g		δ_c, characteristic morphological dimension (nm)
Base alloy treated	Weight % of aluminum remaining after leaching	Uncorrected	Based on active outer layer weight	
430 SS[b]	8.3	Unleached	—	—
430 SS	7.0	[a]	—	—
430 SS	5.5	1.2	15	8.6
430 SS	2.7	2.1	29	4.4
430 SS	0.5	1.9	31	4.2

[a] Below sensitivity of apparatus.

[b] 430 SS composed of 80% Fe and 20% Cr.

were conductive, they could then be inserted directly into the ETEC Model U-1 SEM without further treatment. Each wire was fully scanned to find a representative area for micrographs. Micrographs from 100 to 10,000 magnifications were obtained.

Sample preparation for the microprobe required mounting wires on end in a sample holder. The wires were held in place by an epoxy resin. After setting in the epoxy resin, wire ends were clipped near but not at the epoxy–wire interface. Then followed a series of polishing steps which lead to a very fine, smooth, cross-sectional surface of each wire. The final polishing material used was 0.3-μm alumina. The polished surface when viewed under an optical microscope showed an almost perfectly smooth surface. Once polished, the sample holder with the cross sections was carbon coated. The holder was then placed into the microprobe for the evaluation discussed below. The microprobe was an ETEC Autoprobe sensitive to elements from sodium upward in molecular weight. Multiple wavelengths corresponding to different elements could be scanned simultaneously. Calibration was done with standards placed in the Autoprobe along with the specimens. Elemental qualitative analyses (within a volume of 10 μm^3) by line and raster scanning were done with the probe.

Pore size distribution was determined by mercury intrusion with a Quantachrome scanning porosimeter. Even the most active catalyst, 430 SS–0.5% Al, did not have any measurable pores between 2 and 500 nm.

RESULTS

A listing of etched metal catalysts fully evaluated is given in Table 1 along with BET surface areas. Column 1 represents the base alloy activated, column 2 is the weight percentage of aluminum remaining after leaching, and columns 3 and 4 are BET surface areas as defined below. Figure 1, a 100× micrograph, shows the etched metal catalyst with substantial aluminum remaining after mild leaching (430 SS–7.0% Al). Note that the aluminum exists as islands on the surface. The removal process is interesting in itself since it appears to be a highly selective process. The alkali penetrates the aluminum outer layer by forming fissures to the alloy core, then depending upon the degree of exposure, the outer lobes selectively disappear, exposing the alloy core surface. Orchard *et al.* (*7*) have also reported that the mechanism of leaching is one of selective dissolution for Raney nickel–cobalt catalysts.

In Fig. 2, the 430 SS–0.5% Al, a more

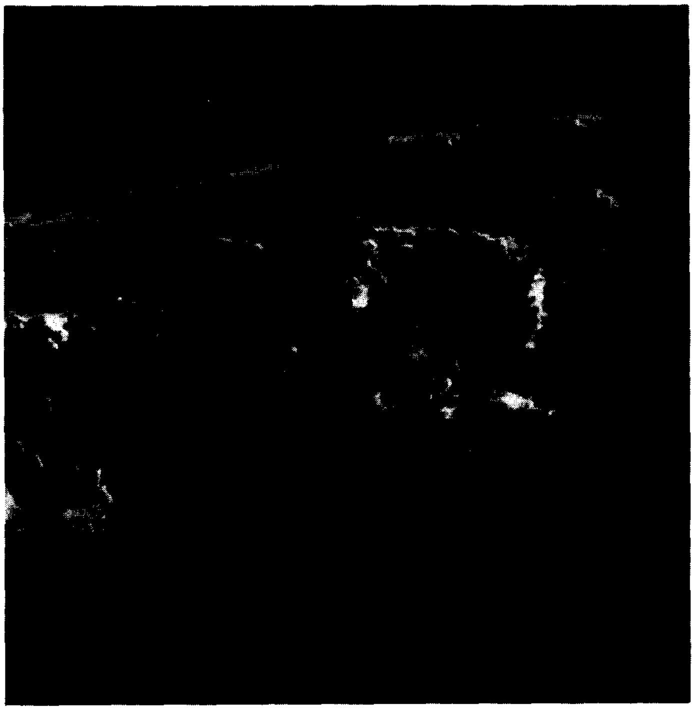

FIG. 1. A 100× micrograph of a 430-SS wire after aluminum diffusion coating and partial leaching (430 SS–7.0% Al).

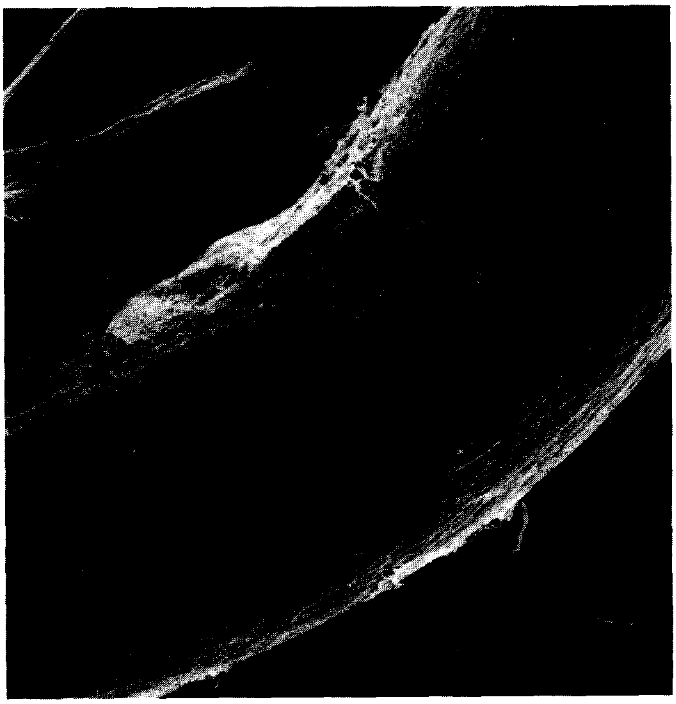

FIG. 2. A 100× micrograph of a 430-SS wire after aluminum diffusion coating and nearly complete leaching (430 SS–0.5% Al).

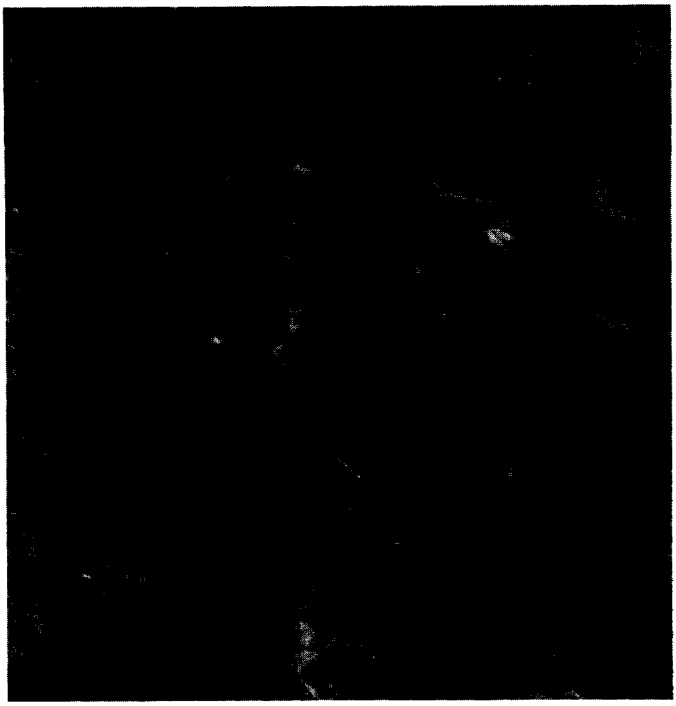

FIG. 3. A 1000× micrograph of an untreated 430-SS Wire.

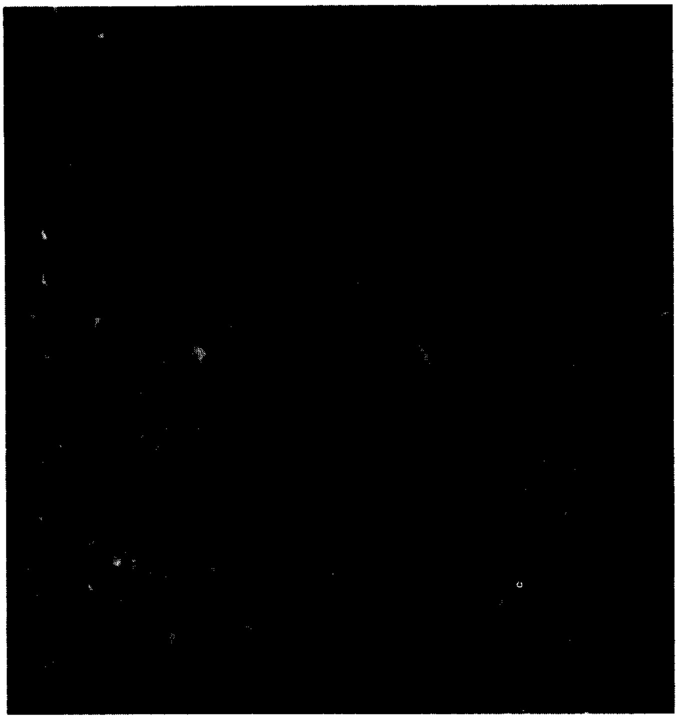

FIG. 4. A 1000× micrograph of a 430-SS wire after aluminum diffusion coating and nearly complete leaching (430 SS–0.5% Al).

severely etched metal catalyst at 100×, shows the islands have disappeared; however, roughened surface texture has developed. The surface texture development is better demonstrated when Fig. 3 (untreated 430 SS) is compared to Fig. 4 (the 430 SS–0.5% Al catalyst). Both of these figures are at a magnification of 1000. The untreated surface is fairly uniform and smooth with only a few imperfections; however, the treated surface has many nodules and platelet disruptions. A discussion of the effect of etching on activity is presented below.

The microprobe further elucidated the diffusional process used to form these catalysts. Single point scans across a cross section of the wire, called elemental line scans, demonstrate the diffusion of aluminum into the 430 SS as shown in Fig. 5. The series on the 430 SS–8.3% Al wire, representing aluminum diffusion but no leaching, show that aluminum diffused in as a wave with very sharp gradients at the aluminum–430 SS boundary. Chromium and iron (the second and third micrographs) appeared to diffuse outward into the aluminum layer. The thickness of the aluminum layer was estimated from these micrographs at 18 μm. Interestingly, the iron concentration shows two discontinuities. This may be the result of the formation of alloy phases between Fe and Al as in the α and β phase formation in the Raney nickel process. Chromium did not show these discontinuities. Orchard *et*

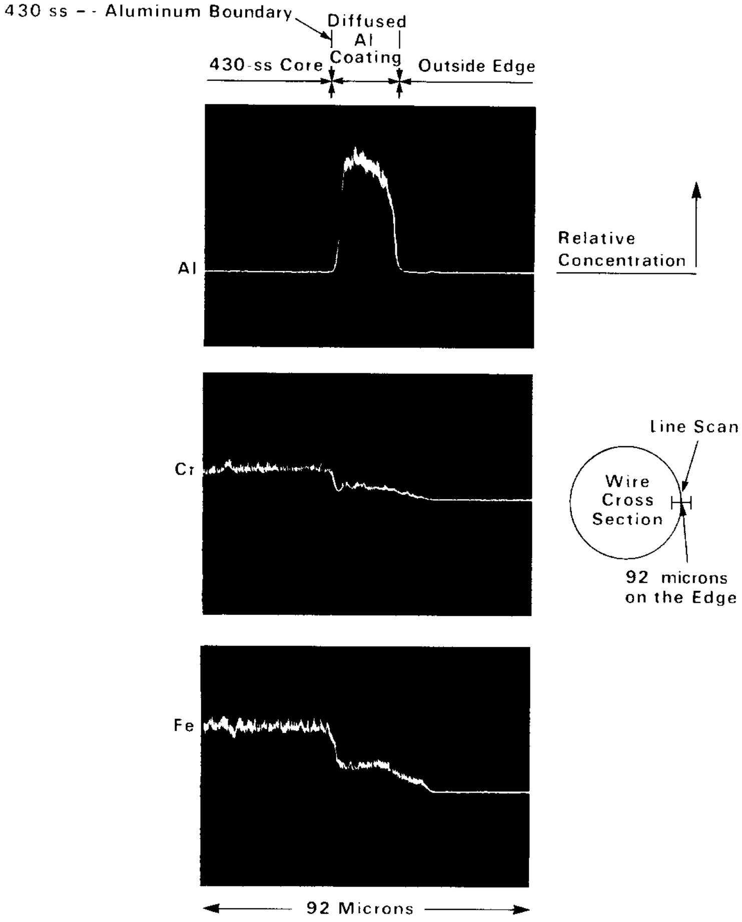

FIG. 5. Microprobe elemental line scans on 430 SS–8.3% Al (unleached).

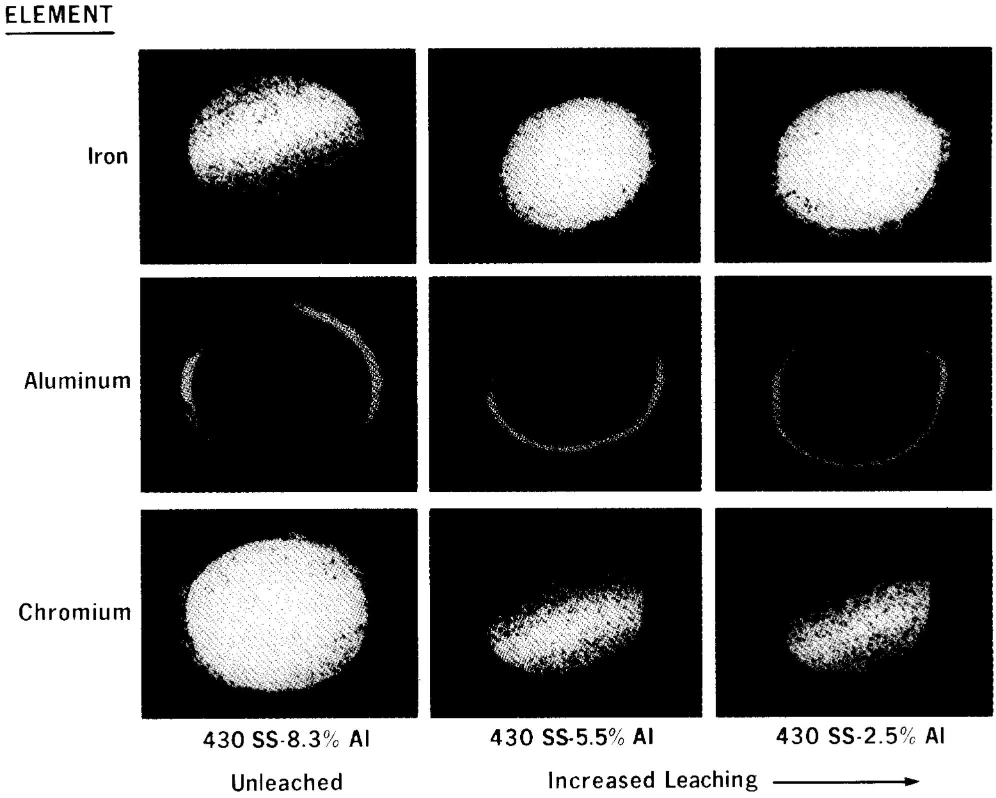

FIG. 6. Microprobe raster scans on cross-sectional etched metal catalysts.

al. (*7*) reported that $NiAl_3$ leached faster than Ni_2Al_3, and that Ni_2Al_3 retained 30% of the initial atomic aluminum present when leached. However, in the case of cobalt, they reported that Co_2Al_5 leached faster than CoAl with both phases losing almost all of their aluminum content. The results of this work suggest similarities with Raney cobalt alloys.

Figure 6 shows a composite of raster scans. The composite is made up of three elemental raster scans, iron, aluminum, and chromium, for three of the five etched metal catalysts listed in Table 1. The series shows increased leaching from left to right. The composite shows that as etching increased, the aluminum ring layer (middle row) became thinner. For a nearly fully leached sample (at right end), only a thin aluminum ring remains on the outside edge. The outer edge also showed rings of iron (top row) and chromium (bottom row) which had lower intensity, and thus lower weight percentage, compared with the bulk. This supports the conclusion from the line scans that iron and chromium back-diffuse into the aluminum outer layer. It is believed that iron and chromium are not leached away during the leaching process. This may be observed by comparing ring widths of the nearly fully leached aluminum raster scan to those of iron and chromium. The ring for aluminum (middle row, right column) compared to rings for iron and chromium (top and bottom row, right column) is slightly thinner. The small imperfections seem to be due to the clipping process and subsequent polishing that removed minute outer layers. Because the microprobe could monitor three characteristic wavelengths simultaneously, all three elements were scanned and recorded at the same time.

The reporting of surface area as square

meter per gram of total weight is inadequate and misleading for catalysts with a solid, inert core covered by a thin layer with catalytic activity and high surface morphology. This is the nature of the etched metal catalysts. The microscopic studies described above reveal that only the outer layer (18 μm) is roughened by etching, creating cracks and fissures. The inner core is impervious and catalytically inert. The area per gram of outer active layer can be estimated based on the thickness and density of the measured composition of that layer. This active surface area is calculated excluding the impervious core, i.e.,

Corrected BET = Measured BET/Weight fraction of catalyst in the outer active layer

$$\text{Weight fraction of catalyst in outer active layer} = \frac{(r_o^2 - r_i^2)\rho_o}{r_i^2\rho_i + (r_o^2 - r_i^2)\rho_o}$$

where ρ_i = density of inner core; r_i = radius of inner core; ρ_o = density of outer layer; r_o = radius of Al-coated wire. The results of these corrections are shown in column 4 of Table 1. This corrected area, for the most fully etched catalyst, was about half the measured surface area of a typical Raney nickel (80 m^2/gm) (*8*).

To eliminate the effect of density inherent in reporting surface areas in the traditional BET units, it is useful to calculate the surface area per unit of solid volume of active catalyst, and a characteristic morphological dimension, δ_c, i.e.,

$$\text{Surface area/solid volume} = SA/V = \text{Area(BET)} \times \rho \text{ (solid density)}$$

$$\text{and characteristic morphological dimension } \delta_c = 1/SA/V \text{ (in nm)}.$$

For smooth spheres, $\delta_c = r/3$; and for smooth infinite plates, $\delta_c = r/2$, where r = the radius of the sphere, or half the plate thickness.

On this basis, the most fully etched metal catalyst had a value of $SA/V = 240$ m^2/cm^3, corresponding to $\delta_c = 4.2$ nm. For comparison, a 200 m^2/gm silica has a value of $SA/V = 440$ m^2/cm^3, so $\delta_c = 2.3$ nm. For a 100 m^2/gm alumina, $SA/V = 400$ m^2/cm^3 and $\delta_c = 2.5$ nm. Materials with identical morphology, i.e., both size and shape, will have the same value of SA/V and hence δ_c, regardless of density. As an example, values of $SA/V = 400$ m^2/cm^3 and $\delta_c = 2.5$ nm will be created by 7.5-nm spheres, or platelets 5.0-nm thick (neglecting edge effects), independent of the material. Thus, the morphology created by the etching process is comparable in its values of SA/V and δ_c to moderate surface area silicas and aluminas.

ACTIVITY COMPARISON

Sets of etched metal catalyst screens of each of the five compositions described in Table 1 were mounted in parallel passage reactor cartridge configuration and evaluated as catalysts for Reaction (1). Each individual screen was 4.44 cm wide and 20.32 cm long. Each reactor cartridge was assembled from six screens, spaced with 7.0-mm gaps. The activity test consisted of measuring NO conversion as a function of temperature at a constant mass flow rate corresponding to a space velocity of 17,000/hr at STP. Feed gas concentrations were 500 ppm NO and 550 ppm NH_3 in flue gas generated from a furnace burning No. 2 oil. Gas flow was parallel to the screens, downward through the 7-mm gaps.

Results, presented in Fig. 7, showed the most fully etched screens (430 SS–0.5% Al) to have the highest activity. Under the conditions used, a maximum of 65.8% in the conversion occurred at 715 K. These conditions corresponded to a reactor space velocity at reactor temperature and pressure of 43,000/hr, or a residence time of 0.084 S.

The results also showed a clear trend of activity increasing with the degree of etching. Screens of 430 SS–8.3% Al (unleached) showed no activity toward the desired reaction. Screens of 430 SS–7.0% to 0.5% Al, representing progressive leaching, showed activity improving for each in the series. A

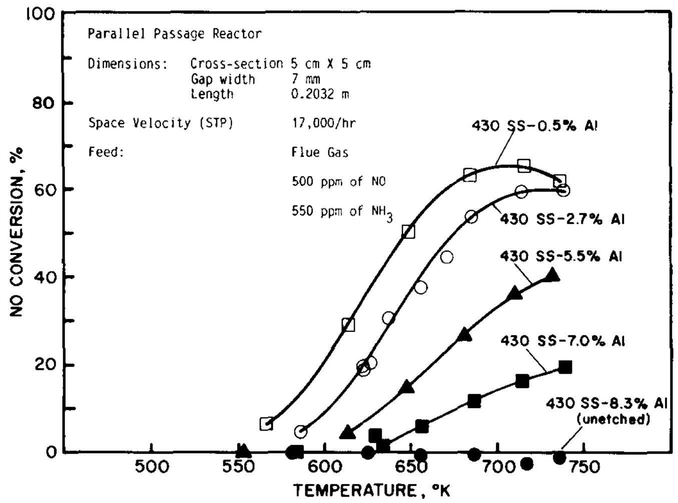

FIG. 7. Performance comparison of 430 SS screens. Effect of degree of etching.

near linear relationship between NO conversion and level of aluminum remaining was found for temperatures below 675 K.

Recent work (*9*) has shown that activity does pass through a maximum with decreasing aluminum content. Not only does the aluminum serve as a medium to create surface area, but chemical surface effects are involved which are related to that remaining aluminum being present. This has also been reported in (*8*) for Raney nickel.

The fully leached etched metal catalyst has undergone further investigation (*3*) which enabled the comparison of its intrinsic surface rate constant with those of two excellent deNO$_x$ catalysts evaluated in similar parallel passage reactor configurations (*10*). These two catalysts, copper on mordenite and vanadia on alumina, listed in Table 2, show lower intrinsic rate constants than the fully leached etched metal catalyst. Since these rate constants are based on the superficial, "flat plate" surface areas of the catalysts in their parallel passage reactor configurations, the BET surface area is not involved in these calculation. However, the etched metal catalyst is dramatically superior based on such catalytic surface area, since the two supported catalysts have BET-type areas between one and two orders of magnitude greater than the etched metal catalyst, per square centimeter of superficial, "flat plate" area. The two supported catalysts used were of a particle size of 50–100 mesh. Nam (*11*) has determined that 20/30 mesh catalyst of the same com-

TABLE 2

Comparison of Relative Activity of NO$_x$ Catalysts at 644 K

Catalyst	Apparent first-order rate constant, k_s (m/hr)
Copper on mordenite	93.6
Vandia on alumina	86.4
430 SS–0.5% Al ETM screens	197.1

Note. This area-based rate constant is used in the kinetic equation for parallel passage reactors:

$$r_{NO} = k_s C_{NO},$$

where

$$r_{NO} = \frac{\text{moles of NO reduced}}{\text{hr} \cdot \text{m}^2 \text{ of superficial ``flat plate'' catalysts area}}$$

and

$$C_{NO} = \frac{\text{moles of NO}}{\text{m}^3} \text{ in gas phase.}$$

position has an effectiveness factor over 0.90 and that the smaller particles (50–100 mesh) would thus have a higher effectiveness factor. Thus, intraparticle mass transfer limitations are minimal in this comparison.

ACKNOWLEDGMENTS

The authors acknowledge the assistance of the University of Massachusetts Geology Department and Polymer Science and Engineering Department in performing the microprobe and SEM micrograph work. Special thanks to M. David Leonard and Louis Raboin, the technicians involved. The authors also thank Professor James R. Kittrell for his review of the manuscript and suggestions. Finally, this work was done under the sponsorship of Northeast Utilities Service Company, Hartford, Connecticut and Alloy Surfaces Company, Inc. of Wilmington, Delaware.

REFERENCES

1. Freel, J., Pieters, W. J. M., and Anderson, R. B., *J. Catal.* **16,** 218 (1970).
2. Baldi, A. L., and Damiano, V. V., U.S. Patent 4,292,208 (1981).
3. Willey, R. J., Ph.D. dissertation, University of Massachusetts, Amherst, Mass., 1984.
4. Baldi, A. L., and Damiano, V. V., U.S. Patent 4,154,705 (1979).
5. Baldi, A. L., and Damiano, V. V., U.S. Patent 4,041,196 (1977).
6. Baldi, A. L., and Damiano, V. V., U.S. Patent 3,867,184 (1975).
7. Orchard, J. P., Tomsett, A. D., Wainwright, M. S., and Young, D. J., *J. Catal.* **84,** 189 (1983).
8. Satterfield, C. N., "Heterogeneous Catalysis in Practice." McGraw-Hill, New York, 1980.
9. Kittrell, J. R., personal communication.
10. Ganti, M. P., Ph.D. dissertation, University of Massachusetts, Amherst, Mass., 1980.
11. Nam, I. S., Ph.D. dissertation, University of Massachusetts, Amherst, Mass., 1983.